

# Machine Learning-Based Adaptive Receive Filtering: Proof-of-Concept on an SDR Platform

Matthias Mehlhose\*, Daniyal Amir Awan†, Renato L. G. Cavalcante\*†, Martin Kurras\* and Slawomir Stanczak\*†

\* *Fraunhofer Institute for Telecommunications, Heinrich Hertz Institute (HHI)*

Department of Wireless Communications and Networks, Einsteinufer 37, 10587 Berlin, Germany  
{matthias.mehlhose, renato.cavalcante, martin.kurras, slawomir.stanczak}@hhi.fraunhofer.de

† *Technical University Of Berlin, Faculty IV - Electrical Engineering and Computer Science*

Department of Telecommunication Systems, Einsteinufer 27, 10587 Berlin, Germany  
{daniyal.a.awan, renato.cavalcante, slawomir.stanczak}@tu-berlin.de

**Abstract**—Conventional multiuser detection techniques either require a large number of antennas at the receiver for a desired performance, or they are too complex for practical implementation. Moreover, many of these techniques, such as successive interference cancellation (SIC), suffer from errors in parameter estimation (user channels, covariance matrix, noise variance, etc.) that is performed before detection of user data symbols. As an alternative to conventional methods, this paper proposes and demonstrates a low-complexity practical Machine Learning (ML) based receiver that achieves similar (and at times better) performance to the SIC receiver. The proposed receiver does not require parameter estimation; instead it uses supervised learning to detect the user modulation symbols directly. We perform comparisons with minimum mean square error (MMSE) and SIC receivers in terms of symbol error rate (SER) and complexity.

**Index Terms**—NOMA, 5G, machine learning, MMSE, multiuser detection

## I. INTRODUCTION

To fulfill the requirement of *massive connectivity* in 5th Generation (5G) mobile networks, highly efficient and flexible use of time and frequency resources is necessary. Current mobile networks mostly employ orthogonal multiple access (OMA) radio access techniques such as orthogonal frequency-division multiple access (OFDMA). In these systems, at each base station (BS), a scheduler allocates resources to each user so as to avoid strong interference from other users. However, the *massive connectivity* requirement in 5G means that the number of simultaneously transmitting devices in the uplink is expected to exceed the number of available orthogonal resources. Therefore, recently a significant body of research has proposed non-orthogonal multiple access (NOMA) [1]–[9]. In these systems, users are allowed to share resources (and thus interfere) and *multiuser detection* techniques [10] are employed to perform reliable detection of user symbols in the uplink. It is well-known that, though the optimal multiuser receiver (in terms of bit error rate (BER)) is nonlinear [10], if the number of antennas at the BS receiver exceeds the number of users, then low-complexity linear receivers (e.g., the MMSE receiver) often show a good performance. However, in *massive connectivity* scenarios, a very large number of antennas at the

receiver are required to achieve a good performance using linear techniques. Furthermore, it is well known that massive antenna systems suffer from various problems such as pilot contamination [11]. Therefore, the assumption that the number of antennas at the BS will be larger than the number of users may not be realistic. In this case, nonlinear detection methods have to be considered. In this study, we demonstrate a promising machine learning based nonlinear multiuser receiver (see [12]) that does not require explicit knowledge of desired or interfering user channels or powers. Furthermore, all users are detected in parallel and independently, and the technique has a relatively low complexity.

### A. The Motivation for a Machine Learning Receiver

As mentioned above, it is known that the optimal detector is the (nonlinear) maximum a-posteriori (MAP) detector [13]. Unfortunately, the MAP detector requires exact knowledge of user channels, their transmit powers and variance of system noise. Estimation of these parameters adds considerable complexity to the receiver design and their estimation is subject to errors. As a compromise, suboptimal nonlinear receivers such as the SIC receiver and those based on neural networks have been proposed [13]–[15]. However, these receivers also require a good estimation of the above mentioned parameters and their complexity becomes impractical for a large number of users. Due to these issues with conventional receiver design, [12] proposed a ML based technique that simplifies receiver design by using supervised learning to detect the desired user symbols directly without any intermediate parameter estimation. It has been shown in [12] through simulations that this technique outperforms the MMSE-SIC receiver (even in the case of exact parameter knowledge) when the number of users exceeds the number of antennas at the BS. Furthermore, this technique works with a relatively small training set which is an important requirement (especially, in the physical layer) in dynamic wireless environments. In the following, we present the multiuser receive filtering model of [12] that we implement and demonstrate in the study.

### B. Multiuser Receive Filtering Model

In the uplink setup,  $K \in \mathbb{N}$  symbol-synchronized users transmit to the BS equipped with  $M \in \mathbb{N}$  antennas at the same frequency. Assuming a non-dispersive channel and symbol-time sampling at time  $t \in \mathbb{N}$ , we can write the received baseband signal as

$$\mathbf{r}(t) = \sum_{k=1}^K \sqrt{p_k(t)} b_k(t) \mathbf{h}_k(t) + \mathbf{n}(t) \in \mathbb{C}^M \quad (1)$$

where  $\mathbf{h}_k(t) \in \mathbb{C}^M$ ,  $b_k(t) \in \mathbb{C}^M$ , and  $p_k(t) \in \mathbb{C}^M$  is the channel, the information-bearing symbol, and the transmit power, respectively, of the  $k$ th user, and where  $\mathbf{n}(t) \in \mathbb{C}^M$  denotes additive noise plus interference from unknown transmissions. The job of baseband receive-filtering is to detect the modulation symbol  $b_k(t)$  of each desired user given  $\mathbf{r}(t)$ .

The online adaptive filtering algorithm of [12] performs the receive filtering for each desired user independently in parallel. In more detail, data communication is preceded by a training phase in which desired users transmit sequences  $(\forall k \in \overline{1, K})$   $(b_k)_{t \in \overline{1, T_{\text{length}}}}$ , where  $T_{\text{length}}$  denotes training time, to the BS. Suppose we are detecting user  $k = 1$ , then the algorithm has access to the training data  $(b_1(t), \mathbf{r}(t))_{t \in \overline{1, T_{\text{length}}}}$ . The training is performed by an adaptive projection subgradient method (APSM) [16] based algorithm. Since this algorithm operates in a reproducing kernel Hilbert space (RKHS)  $\mathcal{H}_{\text{sum}}$ , consisting of weighted linear and nonlinear functions, most operations required by APSM training are carried out via inner products. Therefore, the algorithm has a low complexity. During training  $T_{\text{length}}$ , and for the  $k$ th user, the algorithm learns a nonlinear filter  $f \in \mathcal{H}_{\text{sum}}$  such that

$$(\forall t \in \mathbb{N}) |f(\mathbf{r}(t)) - b_k(t)| \leq \epsilon, \quad (2)$$

where  $\epsilon > 0$  is a sufficiently small (typically  $\epsilon = 0.01 - 0.1$ ) design parameter tuned such that correct hard-detection of  $b_k(t)$  is possible. For sufficiently large training symbols  $T_{\text{length}}$ , and under certain assumptions [16], [17], the algorithm obtains a good estimate of an  $f^* \in \mathcal{H}_{\text{sum}}$  satisfying (2). For more details, see [12].

### C. Contribution and Paper Structure

We summarize the contributions of this study in the following:

- 1) In our *hardware-in-the-loop* setup, we demonstrate our proposed ML based multiuser receiver that is a simpler yet powerful alternative to conventional multiuser receivers.
- 2) We compare the performance of our receiver with the linear MMSE and the nonlinear MMSE-SIC receivers. We show that our receiver outperforms MMSE and it shows comparable (and at times better) performance to MMSE-SIC. Furthermore, we demonstrate that this receiver has a low complexity.

The remainder of the study is organized as follows. In Section II, we present our receiver design including the hardware equipment that we employ during the demonstration and the

signal processing. In Section III, we present our results and perform comparisons with conventional techniques. Section IV concludes this study.

## II. EXPERIMENT SETUP

This section provides the technical details of the hardware and software components being used for our NOMA enabled Software-Defined Radio (SDR) *hardware-in-the-loop* setup.

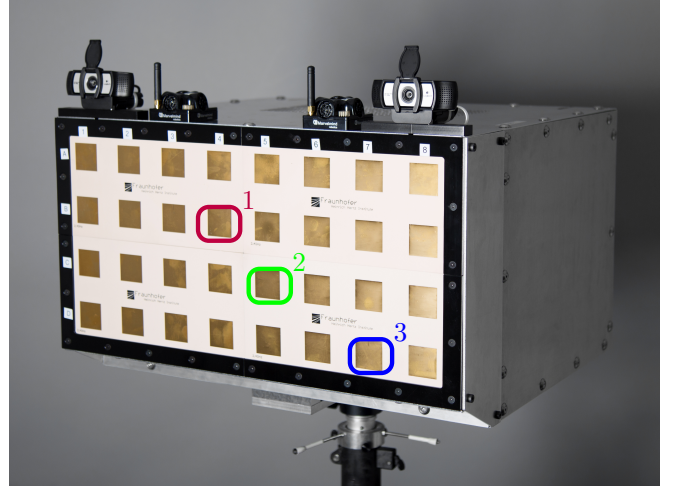


Fig. 1: BS WLAN UPA Array

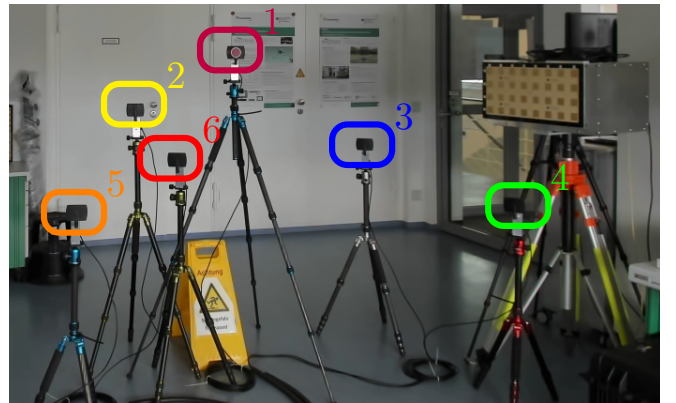


Fig. 2: Demo Setup

### A. Equipment

1) *Software-Defined Radio*: On the digital side of our SDR a Xilinx Zynq XC7Z045 system on chip (SoC) module is mounted. This SoC combines both a Linux running dual ARM Cortex-A9 core pack and field-programmable gate array (FPGA), well equipped to handle both the control and the signal processing tasks. On the analog side, four independent Analog Devices AD9361 are used, each containing an integrated two transceiver path 12-bit analog-to-digital converter (ADC) and digital-to-analog converter (DAC) solution. Each SDR module [18] has eight antenna connections for the transmission and reception direction, respectively. All SDR modules are able to share a 10 MHz reference clock.

2) *Base Station*: The array antenna, shown in Figure 1, is equipped with 32 equidistant cross-polarized patch antenna elements arranged in 4 rows and 8 columns on a planar printed circuit board. Each patch element of this array operates at a center frequency of 2.442 GHz, which correspond to Wireless Local Area Network (WLAN) channel 7. The element spacing is  $\lambda/2$ , where  $\lambda = 12.28$  cm refers to the wavelength at resonant frequency  $f = 2.442$  GHz, and the length and width of each quadratic patch element is  $\lambda/4$ . Each antenna housing has space for up to four SDR modules. The BS parameters are summarized in table I.

TABLE I: BS Parameters

parameter	value	comment
resonant frequency	2.442 GHz	
element spacing	6.14 cm	$\lambda/2$ at 2.442 GHz
element length and width	3.07 cm	$\lambda/4$ at 2.442 GHz
number of rows	4	
number of columns	8	
polarization	H and V	vertical is used
number of SDR modules	up to 4	
number of module antenna ports	8	4x AD9361

3) *User Equipment*: Each of the six user equipments (UEs), shown in Figure 2, is equipped with a commercial off-the-shelf (COTS) WLAN antenna which is connected to one of eight SDR module transmitter ports. According to the datasheet of the manufacturer, the measured antenna gain is 5 dBi at 2.5 GHz and up to 7 dBi at 5.7 GHz and the polarization is vertical.

### B. Signal Processing

In the demonstration, we use an SDR based transceiver connected to a subset of patch antennas arranged as a uniform planar antenna (UPA) array with four rows and eight columns at the receive side. On the transmit side we use a single SDR connected to all users. Each transmit port is connected to a single-antenna user. Table II sums up the demonstration system parameters. The raw time data IQ-buffers from each SDR are transmitted and received over a 1 Gbit Ethernet interface on each SDR module. Transmit signal creation for the users and received signal processing is done on a standard desktop personal computer (PC). The system architecture of the transmit and receive path is shown in Figure 3.

1) *Transmit Signal Chain*: On the transmit side binary phase-shift keying (BPSK) symbols at each user are filtered by a raised cosine transmit filter with an oversampling factor of 16 to avoid excessive multipath transmissions. The training sequence  $(b_k)_{t \in [1, T_{\text{length}}]}$  and the data sequence  $(b_k)_{t > T_{\text{length}}}$  (see Section I-B) are separated by a *Frank-Zadoff-Chu* sequence that is used for time synchronization on the receive side.

2) *Receive Signal Chain*: On the receive side, we receive an IQ buffer twice the size of the transmit buffer size. During each run of the *hardware-in-the-loop* experiment, the filled receive buffer contains a full radio frame of training, synchronization, and data sequences and parts of the preceding and following radio frames. We perform a cross-correlation based time-synchronization to find the position of a complete frame and

extract the superimposed received signals corresponding to the training and data sequences from each user. Both sequences are then filtered with a raised cosine receive filter and sub-sampled by a factor of 16. The first part of this filter output is used to train the ML algorithm and the second part is used to detect the BPSK symbols. Finally, we compare the bit sequence in the binary sink with the bit sequence from the binary source to calculate the SER for each user. Note that we can only measure the SER over the length of the SDR buffer.

TABLE II: Proof-of-Concept System Parameters

parameter	value	comment
carrier frequency	2.442 GHz	WiFi Band 7 (tune able)
system bandwidth	30.72 MHz	
NOMA bandwidth	1.92 MHz	oversampling by a factor of 16
NOMA waveform	BPSK	Single-Carrier Modulation (SCM)
BS height	$\approx 1.5$ m	
number of rx antennas	3	see Figure 1
number of tx antennas	$\leq 6$	see fig. 2 (active users)
user transmit power	-15 to 0 dBm	difference of 3 dB between users
user height distribution	0.8 to 1.8 m	
distance BS and users	2.6 to 4.0 m	
training symbols	$\leq 685$	default: 500
data symbols	$\leq 3840$	default: 3000

## III. DEMONSTRATION RESULTS

In this section, we present the performance of our *hardware-in-the-loop* demonstrator. We compare the performance of the ML-based multiuser receive filtering (see Section I-B), which we denote by Non-Linear (NL)-ML in the following, with:

- the linear MMSE receive filtering in which each user is detected in parallel, and
- the nonlinear MMSE-SIC receiver. In MMSE-SIC, each user is first detected using MMSE filtering and then its contribution is subtracted from the received signal (1) before the next user in the SIC-chain is detected.

### A. Demonstration Setting

As mentioned in Section I-B the data communication is preceded by a training phase of length  $T_{\text{length}}$  complex signals. This training sequence is used to train the NL-ML algorithm and also to perform channel and covariance matrix estimation for MMSE filtering. We use Algorithm 1 in [12] to perform training for each user in parallel. The important parameters are shown in Table III and other parameters were chosen as in [12]. There are  $K = 6$  desired users in the system and we use  $M = 3$  antennas at the BS. In order to multiplex the users in the power domain, as required in power-domain NOMA, each successive user transmits with 3 dB less power.

TABLE III: NL-ML Parameters

User	$w_L$	$w_G$	$T_{\text{length}}$	$D_{\text{length}}$
1	60%	40%	10	3000
2	60%	40%	70	3000
3	60%	40%	40	3000
4	60%	40%	40	3000
5	60%	40%	685	3000
6	60%	40%	685	3000

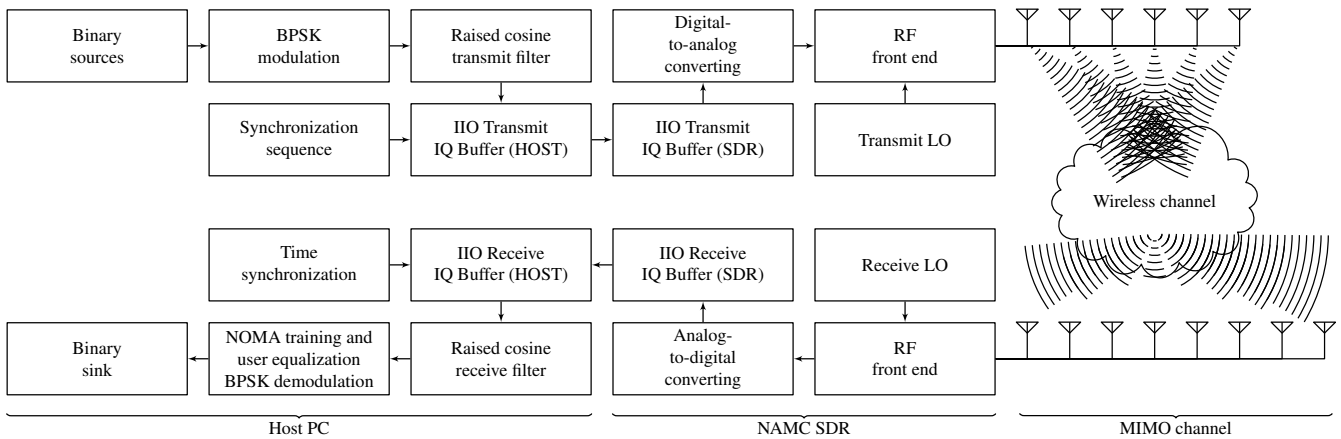


Fig. 3: System Model

### B. Comparison with MMSE and MMSE-SIC

In this section we compare the SER and complexity performance of NL-ML with that of the MMSE and MMSE-SIC. As mentioned above, users are separated in the power domain where user 1 is the “strongest” user and user 6 is the “weakest” user in the system. In terms of the SER, we observed that all 3 techniques showed a comparable near-perfect performance for the first 4 users, i.e.,  $SER \approx 0$  over the observable test sample set (which was restricted to a size of 3000 symbols). Therefore, we omit the results for these users.

In the following, we show the performance for the 5th and the 6th users (which can be thought of as weak users) in terms of the SER and complexity of detection (that we measure in terms of the processing delay). Note that, due to the limited size of the SDR buffer, we can only observe the detection errors for 3000 symbols. Therefore, the minimum observable non-zero SER is  $3.33 \times 10^{-4}$ . Additionally, we show the performance of the overall system in terms of the average SER and average complexity/delay.

Figure 4 and Figure 5, show the SER results for the 5th and the 6th user, respectively. We see that the MMSE shows a poor performance in both cases because these users are linearly inseparable and they suffer from excessive interference from other users. In contrast, the MMSE-SIC and NL-ML show a good and comparable performance in this case. Figure 8 shows the average SER of the system. We see that both MMSE-SIC and NL-ML show a good performance, where NL-ML slightly outperforms MMSE-SIC.

Figure 6 and Figure 7, show the complexity (measured in terms of detection delay) results for the 5th and the 6th user, respectively. We see that the MMSE has low complexity because it is a linear technique. Even though NL-ML is a nonlinear technique, one of its strengths is that it involves robust linear processing and all users are detected in parallel independently. We see that the complexity of NL-ML is comparable to that of the MMSE technique. As expected, the nonlinear MMSE-SIC has a higher complexity than both MMSE and NL-ML. Figure 9 shows the average complexity of the system where we observe once again that NL-ML receiver

has a low complexity.

In conclusion, the simulation results demonstrate that the NL-ML receiver is capable of achieving the SER performance of nonlinear techniques, while it has a complexity comparable to that of linear techniques.

## IV. CONCLUSIONS

We demonstrated a nonlinear ML based multiuser receiver that can achieve the performance of nonlinear receivers and it has the complexity comparable to linear receivers. The proposed receiver does not require parameter estimation (user channels, powers, noise variance, etc.) as in conventional receivers which is subject to errors. We compared the performance with the standard linear MMSE receiver and also with

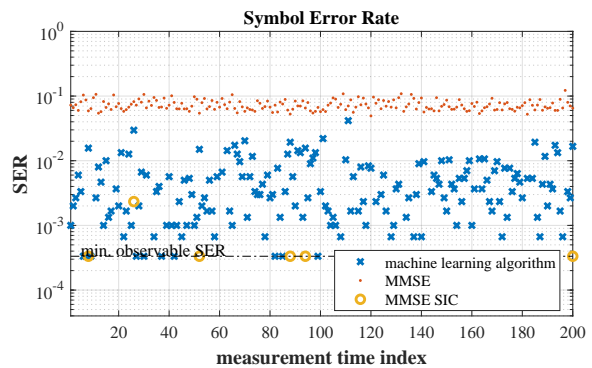


Fig. 4: User 5:  $\omega_L = 0.6$  and  $\omega_G = 0.4$  with  $T_{length} = 685$

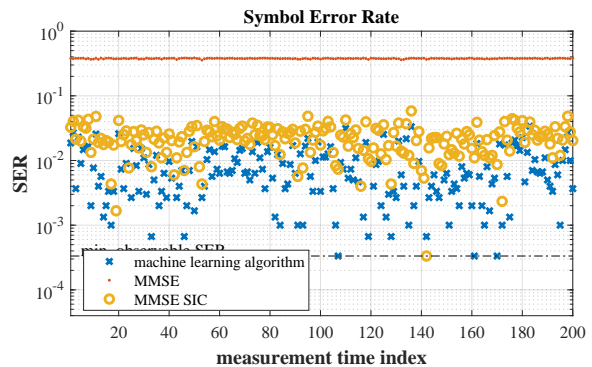


Fig. 5: User 6:  $\omega_L = 0.6$  and  $\omega_G = 0.4$  with  $T_{length} = 685$

the nonlinear MMSE-SIC in a hardware-in-the-loop system. The results show that the proposed ML based multiuser is simpler yet powerful alternative to conventional nonlinear receivers.

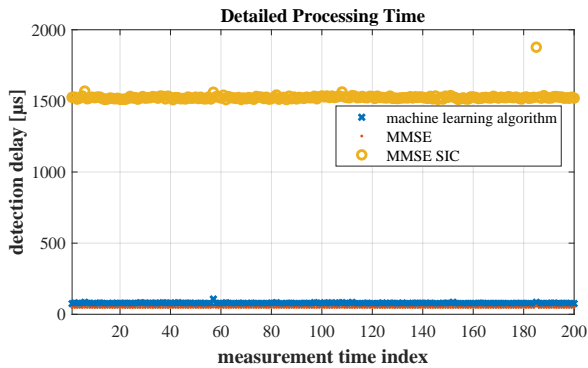


Fig. 6: User 5:  $\omega_L = 0.6$  and  $\omega_G = 0.4$  with  $T_{length} = 685$

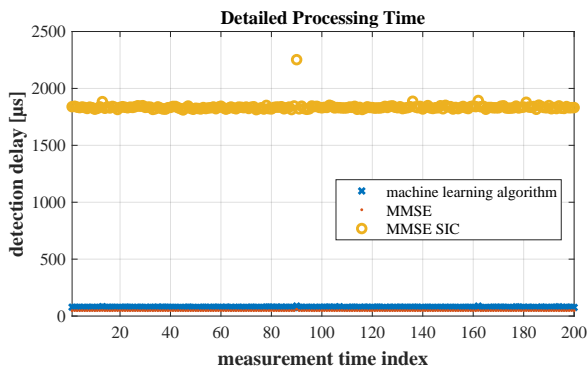


Fig. 7: User 6:  $\omega_L = 0.6$  and  $\omega_G = 0.4$  with  $T_{length} = 685$

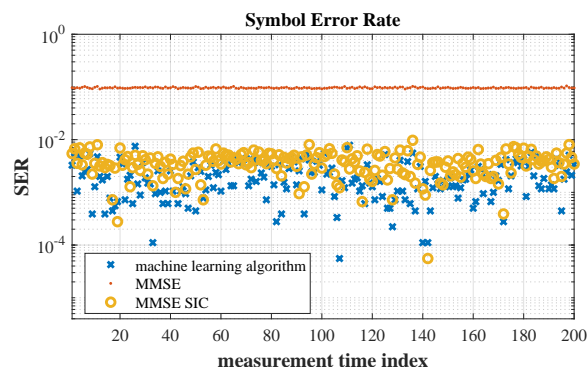


Fig. 8: Mean over all users:  $\omega_L = 0.6$  and  $\omega_G = 0.4$

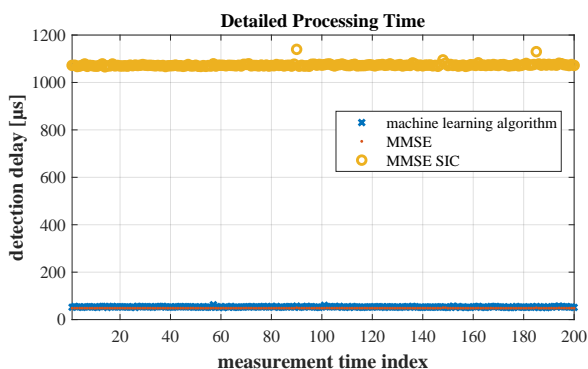


Fig. 9: Mean over all users:  $\omega_L = 0.6$  and  $\omega_G = 0.4$

## ACKNOWLEDGMENTS

The work is supported by the European commission and 5G Infrastructure Public Private Partnership (5G-PPP) and received funding from the EC H2020/5G-PPP program ONE5G (ICT-760809) project [19].

## REFERENCES

- [1] "Study on Non-Orthogonal Multiple Access (NOMA) for NR," 3rd Generation Partnership Project, Tech. Rep. 38.812, Dec. 2018.
- [2] K. Slavakis, S. Theodoridis, and I. Yamada, "Adaptive constrained learning in reproducing kernel hilbert spaces: The robust beamforming case," *IEEE Transactions on Signal Processing*, vol. 57, no. 12, pp. 4744–4764, Dec 2009.
- [3] M. Yukawa, "Adaptive learning in cartesian product of reproducing kernel hilbert spaces," *IEEE Transactions on Signal Processing*, vol. 63, no. 22, pp. 6037–6048, Nov 2015.
- [4] A. Benjebbour and Y. Kishiyama, "Combination of noma and mimo: Concept and experimental trials," in *2018 25th International Conference on Telecommunications (ICT)*, June 2018, pp. 433–438.
- [5] U. S. S. Arachchilage, D. N. K. Jayakody, S. K. Biswash, and R. Dinis, "Recent advances and future research challenges in non-orthogonal multiple access for 5g networks," in *2018 IEEE 87th Vehicular Technology Conference (VTC Spring)*, June 2018, pp. 1–6.
- [6] Z. Ding, X. Lei, G. K. Karagiannidis, R. Schober, J. Yuan, and V. K. Bhargava, "A survey on non-orthogonal multiple access for 5g networks: Research challenges and future trends," *IEEE Journal on Selected Areas in Communications*, vol. 35, no. 10, pp. 2181–2195, Oct 2017.
- [7] W. Cai, C. Chen, L. Bai, Y. Jin, and J. Choi, "Subcarrier and power allocation scheme for downlink ofdm-noma systems," *IET Signal Processing*, vol. 11, no. 1, pp. 51–58, 2017.
- [8] Y. Saito, Y. Kishiyama, A. Benjebbour, T. Nakamura, A. Li, and K. Higuchi, "Non-orthogonal multiple access (noma) for cellular future radio access," in *2013 IEEE 77th Vehicular Technology Conference (VTC Spring)*, June 2013, pp. 1–5.
- [9] S. Abeywickrama, L. Liu, Y. Chi, and C. Yuen, "Over-the-air implementation of uplink NOMA," *CoRR*, vol. abs/1801.05541, 2018. [Online]. Available: <http://arxiv.org/abs/1801.05541>
- [10] S. Verdú, *Multiuser Detection*, 1st ed. New York, NY, USA: Cambridge University Press, 1998.
- [11] O. Elijah, C. Y. Leow, T. A. Rahman, S. Nunoo, and S. Z. Iliya, "A comprehensive survey of pilot contamination in massive mimo—5g system," *IEEE Communications Surveys Tutorials*, vol. 18, no. 2, pp. 905–923, Secondquarter 2016.
- [12] D. A. Awan, R. L. G. Cavalcante, M. Yukawa, and S. Stanczak, "Detection for 5g-noma: An online adaptive machine learning approach," in *2018 IEEE International Conference on Communications (ICC)*, May 2018, pp. 1–6.
- [13] U. Mitra and H. V. Poor, "Neural network techniques for adaptive multiuser demodulation," *IEEE Journal on Selected Areas in Communications*, vol. 12, no. 9, pp. 1460–1470, Dec 1994.
- [14] Y. Isik and T. Necmi, "Multiuser detection with neural network and pic in cdma systems for awgn and rayleigh fading asynchronous channels," *Wireless Personal Communications*, vol. 43, no. 4, pp. 1185–1194, Dec 2007. [Online]. Available: <https://doi.org/10.1007/s11277-007-9293-0>
- [15] B. Aazhang, B. . Paris, and G. C. Orsak, "Neural networks for multiuser detection in code-division multiple-access communications," *IEEE Transactions on Communications*, vol. 40, no. 7, pp. 1212–1222, July 1992.
- [16] I. Yamada and N. Ogura, "Adaptive projected subgradient method for asymptotic minimization of sequence of nonnegative convex functions," *Numerical Functional Analysis and Optimization*, vol. 25, no. 7-8, pp. 593–617, 2005. [Online]. Available: <https://doi.org/10.1081/NFA-200045806>
- [17] S. Chouvardas, K. Slavakis, S. Theodoridis, and I. Yamada, "Stochastic analysis of hyperslab-based adaptive projected subgradient method under bounded noise," *IEEE Signal Processing Letters*, vol. 20, no. 7, pp. 729–732, July 2013.
- [18] N.A.T. GmbH NAMC-SDR. [Online]. Available: <http://www.nateurope.com/products/NAMC-SDR.html>
- [19] 5G-PPP ONE5G. [Online]. Available: <https://5g-ppp.eu/one5g/>